

## Full Moment Tensor Inversion and 3-D Seismic Velocity Structure Analysis of Microearthquake Data in the "WY" Geothermal Field

Hasbi Ash Shiddiqi<sup>1</sup>, Vega Amazona Muchlis<sup>2</sup>, Andri Dian Nugraha<sup>3</sup>, Rachmat Sule<sup>4</sup>

<sup>1</sup>Earth Sciences Graduate Program, Faculty of Earth Sciences and Technology, Institut Teknologi Bandung

<sup>2</sup>Geothermal Engineering, Faculty of Mining and Petroleum Engineering, Institut Teknologi Bandung

<sup>3</sup>Global Geophysical Research Group, Faculty of Mining and Petroleum Engineering, Institut Teknologi Bandung

<sup>4</sup>Applied Geophysical Research Group, Faculty of Mining and Petroleum Engineering, Institut Teknologi Bandung

<sup>1</sup> h.a.shiddiqi@students.itb.ac.id or h.a.shiddiqi@gmail.com

**Keywords:** microearthquakes, waveform inversion, focal mechanism, 3-D seismic velocity structure

### ABSTRACT

A two month microearthquake (MEQ) monitoring was conducted in the "WY" geothermal field during fluid injection in 2005. MEQ data provided information related to processes developed in geothermal reservoirs. In total, 198 MEQ data were analyzed, starting from phase identification to location determination using Geiger's method and ending in joint hypocenter determination. A travel time tomography inversion was performed in order to obtain a better 3-D seismic velocity model with more accurate hypocenter locations, as well as to provide high resolution images of the geothermal reservoir. From the updated velocity model and hypocenter locations, focal mechanisms of 32 MEQ events, which were selected based on hypocenter clustering and signal quality, were analyzed. A full moment tensor inversion algorithm was used. This inversion algorithm utilized MEQ waveforms as data input. The inversion results showed that most of the MEQs had more than 50% non-double-couple components (compensated linear vector dipoles and volumetric). This result may have indicated that those MEQ mechanisms could have possibly been related to steam flow from the southern part of reservoir, which caused the explosive mechanism at the steam zone. Moreover, this possibility was supported by additional information obtained from the  $V_p/V_s$  anomaly zones determined from travel time tomography results, which indicated the existence of steam. Moment tensor inversion results showed positive volume changes at the steam zone in northern part of reservoir and negative volume changes in the southern part of reservoir. In addition, two oblique faults with NE and NNW strike directions were also identified. These faults were combinations of shear fracturing and extensional fracturing.

### 1. INTRODUCTION

Monitoring microearthquakes (MEQs) associated with fluid injection and withdrawal, as well as natural fractures, has been widely used in geothermal fields to obtain important information for reservoir characterization and hazards assessment. The MEQ hypocenter distribution, which is the first step in MEQ analysis, provides one with the knowledge of fluid flow trends. Further analyses include velocity tomography, which provides detailed information on the composition and structure within the reservoir, and focal mechanism solutions, which represent the earthquake mechanism and stress direction.

Earthquake travel time tomography has been successfully applied in tectonics, volcanic centers, and geothermal reservoirs. The velocity structure resulting from tomographic inversion provides information related to geological lithology, structure, and fluids or magmas in the study area. Tomography analysis at the geothermal field scale can resolve shallow structures and low or high velocity anomalies correlated with magmatic or plume intrusion (e.g. Toksoz et al., 2012). Fluid or steam existence can likewise be delineated by tomographic images (e.g. Gritto et al., 2013).

The MEQs mechanisms in volcanic system and geothermal reservoirs resulting from injection and production are incompatible with double-couple mechanism even though this inconsistency is probably associated with poor quality data and modeling defects (Julian et al., 1998).

However, several observations at geothermal and volcanic areas, such as at the Hengil geothermal area in Iceland (Miller et al., 1998), showed that double-couple (DC) and non-double-couple (non-DC) earthquakes coexisted. Thus, these observations led to the suggestion that the non-DC mechanism probably does not come from data and modeling problems. There are two components of the non-DC mechanism: compensated linear vector dipoles (CLVD), which represent the crack that is simultaneously opening and closing in perpendicular direction without a net volume change (Kirkpatrick et al., 1996) and an isotropic component, which represents an explosion or implosion involving volume change (Vavryčuk, 2001).

The "WY" geothermal field is a volcanic hydrothermal system associated with several andesitic volcanic domes. MEQ monitoring was conducted in 2005 to observe the current reservoir dynamics conditions. Thus, 17 seismometers were deployed around the "WY" geothermal field for sufficient coverage.

### 2. DATA AND METHODS

The authors carefully picked P and S arrival times before locating the hypocenter using the Geiger Adaptive Damping code (Nishi, 2005), which employed Geiger's method with adaptive damping scheme. An initial 1D velocity model was derived using the Velest code (Kissling et al., 1994), which utilized the 1D local tomography method and joint hypocenter determination simultaneously. In this processing step, MEQs with azimuthal gap values greater than  $180^\circ$  were excluded in order to acquire a more accurate 1D

velocity model. In total, 198 MEQ data points, which had azimuthal gap values that were less than  $180^0$ , were utilized in a 3D tomography method using SIMULPS (Thurber, 1993; Evans et al., 1994). MEQ arrival times and updated locations obtained from Velest were used as input for SIMULPS. Grid nodes were determined by seismic ray coverage. In addition, this tomography inversion process updated the hypocenter locations (Figure 1) and the velocity model (Figure 2) at the same time through iterations. As a consequence, hypocenters from the tomography inversion were considered to be more precise than hypocenters obtained from the previous step.

We conducted moment tensor inversion using the ISOLA code (Sokos and Zahradník, 2008), which employed body wave waveforms as input. The ISOLA code was adapted from teleseismic waveform inversion (Kikuchi and Kanamori, 1991) into regional and local earthquake cases. Previous studies had used this code to successfully invert the moment tensor of MEQs, even though this code is mostly used for large to moderate size earthquakes. Examples of this application in volcanic systems and reservoirs include the following: a focal mechanism study of MEQs at the Dobrá Voda area in Slovakia (Fojtíková et al., 2010), and a moment tensor inversion for MEQs at the Haje gas storage (Benetatos et al., 2013), and a moment tensor study of MEQs at the Pyhäsalmi ore mine, Finland (Kühn and Vavryčuk, 2013).

We selected MEQ waveform data based on the signal to noise ratio and MEQ must be recorded at least by 5 stations. As a result, 32 MEQ events were chosen to be inverted. However, the low amplitude of MEQ signals which were lower than the tectonic earthquake signals can produce bias results. Therefore, we have to consider the azimuthal gap of each of MEQs event. A full moment tensor mode was selected in order to get a representation of DC and Non-DC mechanisms. The full moment tensor ( $M$ ) is a summation of DC and Non-DC components that are represented as:

$$M = M_{DC} + M_{CLVD} + M_{ISO} \quad (1)$$

where,  $M_{DC}$  is a double-couple component,  $M_{CLVD}$  is the compensated linear vector dipoles and volumetric, and  $M_{ISO}$  is the isotropic/volumetric component. Frequency band for this inversion is 0.5 to 1 Hz, higher frequency compared to tectonic earthquakes. The updated velocity model from tomographic inversion was used to conduct green function computation. Best optimization of correlation of observed and synthetic seismograms is explored through grid-search analysis.

### 3. RESULTS AND INTERPRETATIONS

In total, 198 MEQs were simultaneously relocated with seismic velocity (Figure 1). Most of MEQs were located at shallow depth, which meant that the tomographic results had better resolution at shallow depths. The MEQs were clustered in the northern part of the geothermal area. This pattern was interpreted to indicate that the injected fluid movement had a flow tendency towards the northern part of the field. The tomographic image at an elevation of 1.5 km above sea level (Figure 2 top) indicated a high  $Vp/Vs$  ratio anomaly in the northern part of the field, which was interpreted to indicate the presence of geothermal brine in the caprock. The image at sea level had a low  $Vp/Vs$  ratio in the northern part of the field, which could be interpreted as a steam reservoir zone (Figure 2 bottom). There was an indication of two faults in Figure 2, with one fault striking northeast and the other fault striking north-northwest.

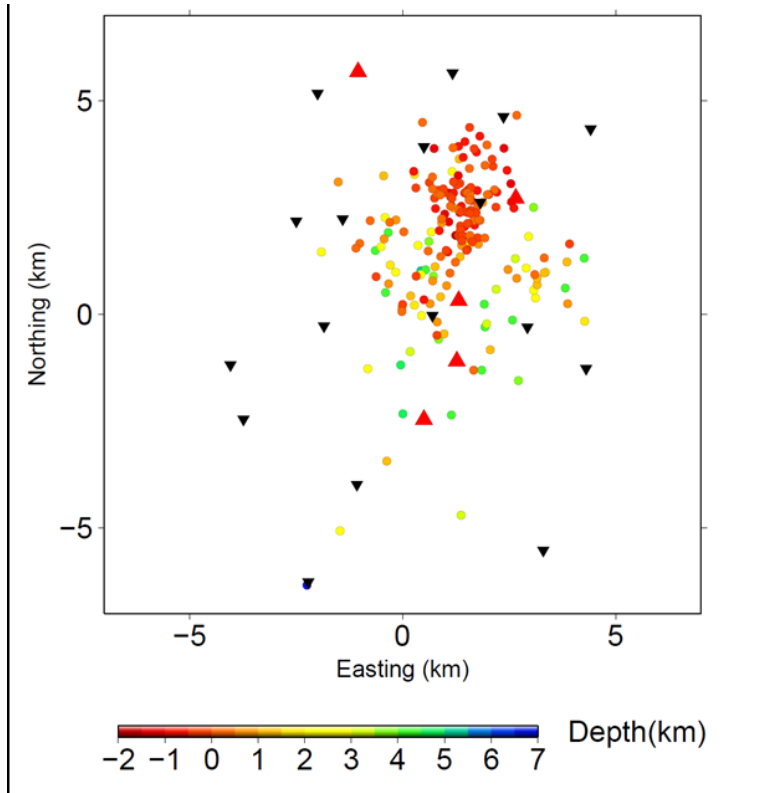


**Figure 1. MEQs relocation distribution at “WY” geothermal area (circle that colored according to their depth relatively to mean sea level), volcanoes are indicated with red triangles, and recording stations are indicated with black reverse triangles.**

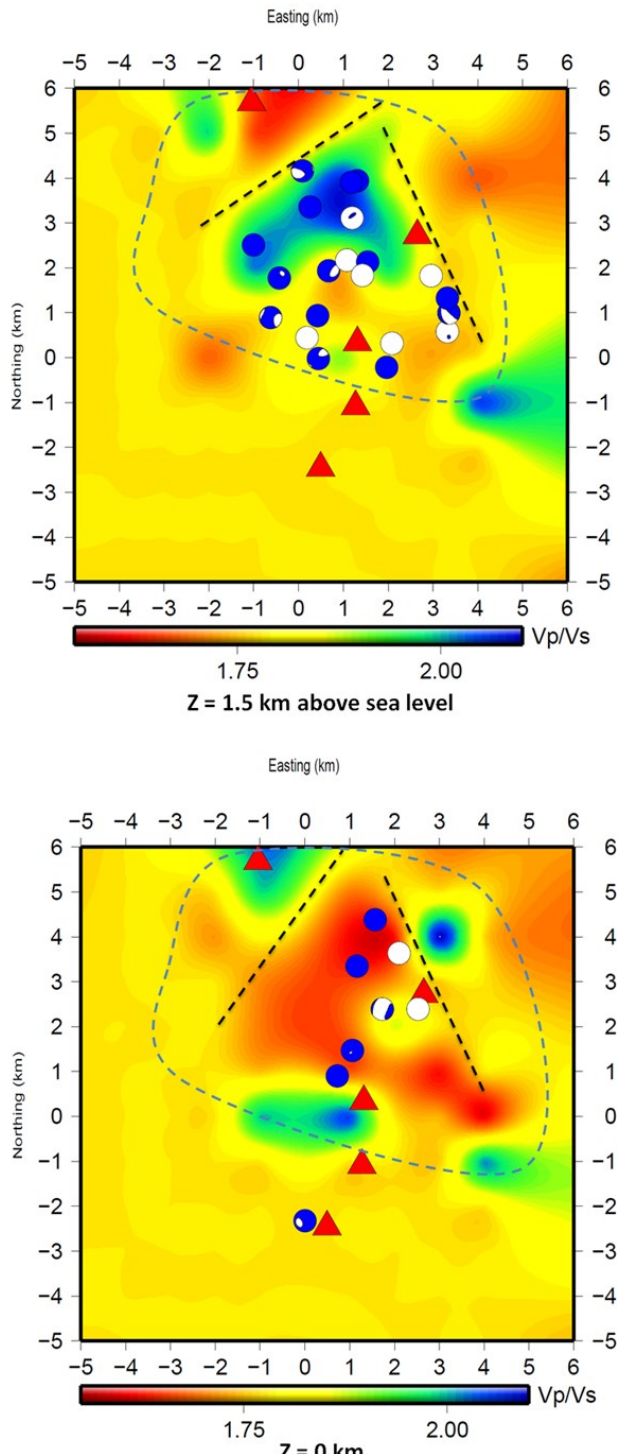


**Figure 2. Top:**  $Vp/Vs$  ratio at 1.5 km above sea level with focal mechanism solutions for event at depth range 2 km to 1 km above sea level. **Bottom:**  $Vp/Vs$  ratio at mean sea level ( $Z=0$  km) with focal mechanism solutions for event at depth range 1 km to -1 km. Volcanoes are indicated with red triangles, recording stations indicated with black reverse triangles, fault indication represented with black dashed line, and area of higher resolution image delineated with blue dashed line.

Moment tensor inversion results, represented with focal mechanism solutions (FMS), were plotted along with the tomography image (Figure 2). Most of FMSs had a dominant isotropic component and minor DC and CLVD components. On the other hand, other FMSs were dominated by deviatoric components (DC and CLVD). Foulger et al. (2004) interpreted isotropic dominated moment tensors to indicate a brisk flow of water or steam that were accompanied with an increase or decrease in volume. At top of Figure 2, FMSs with dominant isotropic components and volume increases (explosive component) (blue circle) were centered in the high  $Vp/Vs$  anomaly zone (geothermal caprock with brine content). Moreover, at the southern part of anomaly, there were several events with an implosive component (isotropic accompanied with volume decrease). Since the caprock is an impermeable rock, it

was assumed that the pattern of those FMSs indicated a rapid flow of steam below the caprock. Furthermore, FMSs plotted at the bottom of Figure 2 indicated a similar pattern, with several explosive mechanisms within the low Vp/Vs anomaly (steam zone).

For patterns of FMSs at this reservoir, it was interpreted that there was fluid flow from the southern part of geothermal area to the northern part. There was also the possibility of a change in the direction of the stress regime in the northern part of the geothermal area. However, this interpretation would need to be supported by another analysis, such as stress inversion. DC components were also found with significant ISO and CLVD components. Two faults that were identified by this study could be interpreted as oblique faults, which are not from pure shear fracturing but also have a extensional fracturing component (Julian et al., 1998; Foulger et al., 2004). This combination of fracturing was possibly a result of high pressure fluid flow at the fracture zone that reduced shear traction (Vavrycuk, 2001).

#### 4. CONCLUSIONS

Results from this study showed that most of the MEQ hypocenters are located at shallow depths of around 0 km to 2 km above sea level and are centered in the northern part of the geothermal area. From the tomographic images, high anomaly Vp/Vs locations were identified, which were interpreted to indicate caprock brine at 1.5 km above sea level. In addition, low anomaly Vp/Vs locations at mean sea level were interpreted to indicate a steam zone. Moment tensor inversion results revealed that an explosive mechanism with positive volume changes dominated the steam zone in the northern part of the reservoir, while an implosive mechanism dominated the southern part. It was interpreted that the steam was flowing from the southern part to the northern part of the geothermal area. Velocity images and FMS values indicated two oblique faults with NE and NNW strike directions and their mechanisms were combinations of shear and extensional fracturing.

#### 5. ACKNOWLEDGEMENTS

The authors gratefully thank the Near Surface Geophysics Laboratory, Faculty of Mining and Petroleum Engineering, ITB. Images in this document were produced using GMT (Wessel and Smith, 1998).

#### REFERENCES

Benetatos, C., Málek, J., and Verga, F.: Moment tensor inversion for two micro-earthquakes occurring inside the Háje gas storage facilities, *Czech Republic, Journal of Seismology*, **17**(2), (2013), 557–577.

Evans, J. R., Eberhart-Phillips, D., and Thurber, H.H.: User's manual for SIMULPS12 for imaging Vp and Vp/Vs: A derivative of the "Thurber" tomographic inversion SIMUL3 for local earthquakes and explosions, *U.S. Geological Survey Open-File Report*, (1994), 94-431.

Fojtíková, L., Vavryčuk, V., Cipciar, A. and Madarás, J.: Focal mechanisms of micro-earthquakes in the Dobrá Voda seismoactive area in the Malé Karpaty Mts. (Little Carpathians), *Tectonophysics*, **492**(1-4), (2010), 213-229.

Foulger, G.R., Julian, B.R., Hill, D.P., Pitt, A.M., Malin, P.E., and Shalev, E.: Non-double-couple microearthquakes at Long Valley caldera, California, provide evidence for hydraulic fracturing, *Journal of Volcanology and Geothermal Research*, **132**(1), (2004), 45-71.

Kühn, D. and Vavrycuk, V.: Determination of full moment tensors of microseismic events in a very heterogeneous mining environment, *Tectonophysics*, **589**, (2013), 33-43.

Gritto, R., Yoo, S.-H., and Jsrpe, S.P.: Three-Dimensional Seismic Tomography at The Geysers Geothermal Field, CA, USA, *Proceedings, Thirty-Eighth Workshop on Geothermal Reservoir Engineering*, Stanford University, Stanford, CA, (2013).

Julian, B.R., Miller, A.D. and Foulger, G.R.: Non-double-couple earthquakes. 1. Theory, *Reviews of Geophysics*, **36**(4), (1998), 525-549.

Kikuchi, M. and Kanamori, H.: Inversion of complex body waves - III, *Bulletin of the Seismological Society of America*, **81**(6), 1991, 2335-2350.

Kirkpatrick, A., J.E. Peterson, Jr., and E.L. Majer.: Source Mechanisms of Microearthquakes at the Southeast Geysers Geothermal Field, California, *Proceedings, Twenty-First Workshop on Geothermal reservoir Engineering*, Stanford University, Stanford, CA, (1996).

Kissling, E., Ellsworth, W.L., Eberhart-Phillips, D., and Kradolfer, U.: Initial reference models in local earthquake tomography, *Journal of Geophysical Research*, **99**(B10), (1994), 19,635-19,646.

Miller, A.D. Foulger, G.R. and Julian, B.R.: Non-Double-Couple Earthquakes 2. Observations, *36*(4), (1998), 551-568.

Nishi, K., 2005.: Hypocenter Calculation Software GAD (Geiger's method with Adaptive Damping), ver.1, **JICA report**, (2005).

Sokos, E.N., and Zahradník, J.: ISOLA a Fortran code and a Matlab GUI to perform multiple-point source inversion of seismic data, *Computers & Geosciences*, **34**(8), (2008), 967-977.

Thurber, C. H.: Local earthquake tomography: Velocities and Vp/Vs-theory, in *Seismic Tomography: Theory and Practice*, H. M. Iyer and K. Hirahara (Editors), Chapman and Hall, London, (1993), 563–583.

Toksöz, M.N., Zhang, H., Benson, T.R., and Rael, A.: Geothermal Resources Exploration and Assessment around the Cove Fort-Sulphurdale Geothermal Field in Utah by Multiple Geophysical Imaging, *Trans. Geothermal Resources Council*, **34**, (2010).

Vavrycuk, V.: Inversion for parameters of "WY" earthquakes, *Journal of Geophysical Research*, **106**, (2001), 16,339–16,355.

Wessel, P., and Smith. W.H. F.: New, Improved Version of the Generic Mapping Tools Released, *EOS Transactions, AGU*, **79**, (1998), 579.